ORIGINAL ARTICLE

DOI: 10.4274/hamidiyemedj.galenos.2024.72692

Hamidiye Med J 2024;5(2):97-105

Breast Ultrasound and Dynamic Contrast-Enhanced Magnetic Resonance Imaging Findings of Idiopathic Granulomatous Mastitis: A Retrospective Single-Center Clinical Study

İdiyopatik Granülomatöz Mastitin Meme Ultrasonu ve Dinamik Kontrastlı Manyetik Rezonans Görüntüleme Bulguları: Retrospektif Tek Merkezli Bir Klinik Deneyim

Filiz Taşçı[1], Yavuz Metin[2], Nurgül Orhan Metin[3], Melih Gaffar Gözükara[4], Erencan Taşçı[5]

[1]*Recep Tayyip Erdoğan University Faculty of Medicine, Department of Radiology, Rize, Türkiye*

[2]*Ankara University Faculty of Medicine, Department of Radiology, Ankara, Türkiye*

[3]*Beytepe Murat Erdi Eker State Hospital, Radiology Unit, Ankara, Türkiye*

[4]*Ankara Distrcit Health Directorate, Ankara, Türkiye*

[5]*Recep Tayyip Erdoğan University Faculty of Medicine, Department of Pediatric Emergency Service, Rize, Türkiye*

ABSTRACT

Background: We aimed to evaluate the effectiveness of breast ultrasound (US) and dynamic contrast-enhanced magnetic resonance imaging (DC-MRI) in the diagnosis of idiopathic granulomatous mastitis (IGM).

Materials and Methods: Breast US and DC-MRI findings of 42 female patients diagnosed with IGM histopathologically were retrospectively evaluated. Patient's age, pregnancy history, symptoms, prolactin level, and Breast Imaging-Reporting and Data System (BI-RADS) category of breast lesions were recorded.

Results: The median age of patients was 39 years (range, 20-71 years, 76.2% were under 40 years of age). Pregnancy history, elevated serum prolactin levels, and complaints (breast pain, swelling, or rash) were evident in 40.5%, 23.8%, and 95.2% of the patients, respectively. Breast lesions were mostly categorized as BI-RADS category 3 (38.1%) or BI-RADS category 4A (40.5%). The most common additional findings detected in both imaging modalities were edema (95.2%; 90.5%), reactive lymph nodes (95.2% each), and skin thickening (90.5%; 52.4%). The most common findings specific to US are lesions with irregular borders (88.1%) and hypo-heterogenic echo pattern (92.9%); tubular expansion and connecting tracts (88.1%), cystic component (69.0%), floating debris (64.3%), and ductal ectasia (52.4%). The most common findings specific to DC-MRI are; localized collective abscess (57.5%) and micro-abscess (53.7%), minimal background parenchymal enhancement (66.6%), non-mass enhancement with heterogeneous (48.3%) or cluster (44.8%) internal pattern, and regional distribution (44.8%). Median values for abscess size, lymph node short axis, and apparent diffusion coefficient were 25 mm, 10 mm, and (1.064x10-3 mm^2/s), respectively, while the mean lymph node long axis was 18.0 mm.

Conclusion: Some findings detected on US (heterogeneous hypoechoic lesions, tubular expansion and connection paths, cystic component, floating debris and ductal ectasia) and breast MRI (regionally distributed heterogeneous or clustered internal pattern, non-mass contrast enhancement and minimal background staining, localized collective abscess or microabscess) largely support the diagnosis of IGM.

Keywords: Idiopathic granulomatous mastitis, breast, magnetic resonance imaging, ultrasonography

Address for Correspondence: Filiz Taşçı, Recep Tayyip Erdoğan University Faculty of Medicine, Department of Radiology, Rize, Türkiye
Phone: +90 533 316 38 19 E-mail: filiztasci@outlook.com **ORCID ID:** orcid.org/0000-0002-8981-171X

Received: 06.01.2024 **Accepted:** 24.05.2024

ÖZ

Amaç: İdiyopatik granülomatöz mastit (İGM) tanısında meme ultrasonu (US) ve dinamik kontrastlı manyetik rezonans görüntülemenin (DK-MRG) etkinliğini değerlendirmeyi amaçladık.

Gereç ve Yöntemler: Histopatolojik olarak İGM tanısı konulan 42 kadın hastanın meme US ve MRG bulguları geriye dönük olarak değerlendirildi. Hastanın yaşı, gebelik öyküsü, semptomları, prolaktin düzeyi ve meme lezyonlarının Meme Görüntüleme-Raporlama ve Veri Sistemi (BI-RADS) kategorisi kaydedildi.

Bulgular: Hastaların ortanca yaşı 39 idi (aralık, 20-71 yıl, %76,2'si 40 yaşın altındaydı). Gebelik öyküsü, yüksek serum prolaktin seviyeleri ve şikayetler (meme ağrısı, şişlik veya kızarıklık) sırasıyla hastaların %40,5, %23,8 ve %95,2'sinde belirgindi. Meme lezyonları çoğunlukla BI-RADS kategori 3 (%38,1) veya BI-RADS kategori 4A (%40,5) olarak kategorize edildi. Çoğu hastada US ve DK-MRG bulguları sol taraflı (sırasıyla %52,4; %57,1), kitlesiz (%69,0; %59,5), düzensiz şekilli (%90,5; %66,7) ve 1-3 kadran yerleşimli (%66,7; %45,2) lezyon olarak tanımlandı. Her iki görüntüleme yönteminde de en sık saptanan ek bulgular ödem (%95,2; %90,5), reaktif lenf nodları (%95,2) ve deri kalınlaşması (%90,5; %52,4) idi. US'ye özgü en sık bulgular, düzensiz sınırları olan (%88,1) ve hipo-heterojenik eko paternli (%92,9) lezyonlara ek olarak; tübüler genişleme ve bağlantı yolları (%88,1), kistik bileşen (%69.0), yüzen debris (%64.3) ve duktal ektazi (%52.4) idi. DK-MRG'ye özgü en yaygın bulgular; lokalize kollektif apse (%57,5) ve mikro-apse (%53,7), minimal arka plan kontrastlanması (%66,6), heterojen (%48,3) veya kümesel (%44,8) iç patern ve bölgesel dağılım (%44,8) ile kitlesel olmayan kontrastlanma. Apse boyutu, lenf nodu kısa ekseni ve görünür difüzyon katsayısı için medyan değerler sırasıyla 25 mm, 10 mm ve (1,064x10-3 mm^2/s) iken, ortalama lenf nodu uzun ekseni 18,0 mm idi.

Sonuç: US (heterojen hipoekoik lezyonlar, tübüler genişleme ve bağlantı yolları, kistik komponent, yüzen debris ve duktal ektazi) ve meme MRG'de saptanan bazı bulgular (bölgesel dağılımlı heterojen veya kümelenmiş iç paternli, kitlesel olmayan kontrastlanma ve minimal zemin boyanması, lokalize kollektif apse veya mikroabse) IGM tanısını büyük ölçüde destekler.

Anahtar Kelimeler: İdiyopatik granülomatöz mastit, meme, manyetik rezonans görüntüleme, ultrasonografi

Introduction

Idiopathic granulomatous mastitis (IGM) is a rare chronic inflammatory breast disease of unknown etiology that primarily affects premenopausal women with a history of pregnancy and lactation (1,2,3). Diagnosis of IGM poses a challenge because of its resemblance to infectious mastitis or inflammatory breast carcinoma both clinically and radiologically (2,3,4,5). Clinical diagnosis, often delayed and achieved through exclusion, can be facilitated by imaging, with radiologists playing a crucial role in suggesting a diagnosis in appropriate clinical contexts (1,2,4,6). Accurate interpretation of imaging results is vital for establishing a timely and definitive diagnosis, which is supported by histopathological examination (2,3,5,6,7). Although traditional radiological modalities like mammography and ultrasound (US) are commonly used for assessing IGM, they often yield non-specific findings such as focal asymmetries, masses, and skin thickening (2,8,9,10). Magnetic resonance imaging (MRI) has emerged as a key diagnostic tool, offering advantages over mammography and US in evaluating various breast conditions (8,10,11). However, initial imaging assessment for IGM typically relies on US because of its predominance in premenopausal women presenting with mastitis symptoms and palpable masses (5). Consequently, the literature on MRI findings associated with IGM is limited, consisting mainly of small case series. Despite normal US findings not excluding IGM, MRI findings may lack specificity because of overlapping features suggesting malignancy or other granulomatous breast disorders (4,11,12,13,14)

In this study, we aimed to evaluate the effectiveness of breast US and dynamic contrast-enhanced magnetic resonance imaging (DC-MRI) in the diagnosis of IGM.

Materials and Methods

Study Population

A total of 42 female patients (median age: 20 years, ranged 39 to 71 years) with confirmed pathology of IGM who underwent breast US and DC-MRI were included in this cross-sectional study conducted between May 2015 and December 2020 in a tertiary care radiology clinic. This study was conducted in accordance with the ethical principles stated in the "Declaration of Helsinki" and approved by Recep Tayyip Erdoğan University Hospital Non-interventional Clinical Research Ethics Committee (date: 21/01/2021; protocol number: 2021/18). Written informed consent was obtained from all patients.

Assessments

Data on the patient's age, history of pregnancy, symptoms (pain, swelling, rash), prolactin level, and Breast Imaging-Reporting and Data System (BI-RADS) category were recorded. US imaging findings [lesion's side, location, shape, echo pattern, margin, fistula to skin, cystic component, floating debris, ductal ectasia, skin thickening, edema, reactive lymph node, nipple retraction, tubular extension and connecting tracts and BI-RADS results) and breast DC-MRI findings (lesion's side, location, type, shape, fistula to skin, micro-abscess, abscess size, localized collective abscess, skin thickening, edema, lymph node long-short

axis, reactive lymph node, nipple retraction, background parenchymal enhancements (BPE), non-mass enhancement (NME) characteristics (internal pattern, lesion distribution type), diffusion restriction and apparent diffusion coefficient (ADC) value] of breast lesions were also recorded.

Imaging Assessments

High-definition US images (LOGIQ P6, GE, USA) were acquired using a linear-array transducer with a central frequency of 7.5 MHz. MRI indications encompassed the exclusion of inflammatory cancer in cases resistant to treatment, further evaluation for patients with inconclusive mammography and/or sonography results, and determination of disease extent. MRI was conducted after conventional examinations in all patients, ensuring no treatment delays occurred. MRI procedures were performed using a 1.5-T whole-body imaging system (Siemens Magnetom Aera Syngo MR D13, Erlangen, Germany) or a 3-T whole-body imaging system (GE Healthcare Discovery MR750, Waukesha, WI).

Statistical Analysis

For statistical analysis, IBM SPSS Statistics for Windows, version 23.0, was used (IBM Corp., Armonk, NY). The assessment of variables' adherence to normal distribution was conducted visually through histograms and probability graphs, and using the Kolmogorov-Smirnov method. Data are presented in terms of mean (standard deviation), median (minimum-maximum), and percentage (%) as deemed appropriate.

Results

Baseline Characteristics

The median age of female patients diagnosed with IGM was 39 years (range: 20 to 71 years), with 57.1% and 76.2% of patients below 40 and 50 years, respectively. Notably, 40.5% had a history of pregnancy, 23.8% showed elevated serum prolactin levels, and 95.2% presented with breast pain, swelling, or rash (Table 1). Most lesions were classified as probably benign (38.1%) or with low suspicion of malignancy (40.5%) (Table 1). US imaging (n=42) predominantly revealed left-sided (52.4%) and non-mass (69.0%) lesions distributed across 1-3 quadrants (66.7%), characterized by irregular shape (90.5%), indeterminate margins (88.1%), and hypo-heterogeneous echo pattern (92.9%). Common associated findings included edema (95.2%), reactive lymph nodes (95.2%), and skin thickening (90.5%) (Figures 1, 2). Nipple retraction or fistula to the skin

Table 1. Baseline characteristics

Age (year)	Mean (SD)	41.9 (12.1)
	Median (min.-max.)	39 (20-71)
Age group, n (%)	≤40 years, n (%)	24 (57.1)
	≤50 years, n (%)	32 (76.2)
Pregnancy history, n (%)	Yes	17 (40.5)
	No	25 (59.5)
Elevated serum prolactin levels (>25 ng/mL), n (%)	Yes	10 (23.8)
	No	32 (76.2)
Breast pain, swelling, rash, n (%)	Yes	40 (95.2)
	No	2 (4.8)
BI-RADS classification, n (%)		
3 (probably benign)		16 (38.1)
4A (low suspicion for malignancy)		17 (40.5)
4B (moderate suspicion for malignancy)		3 (7.1)
4C (high suspicion for malignancy)		6 (14.3)

BI-RADS: Breast Imaging Reporting and Data System, min.: Minimum, max.: Maximum, SD: Standard deviation

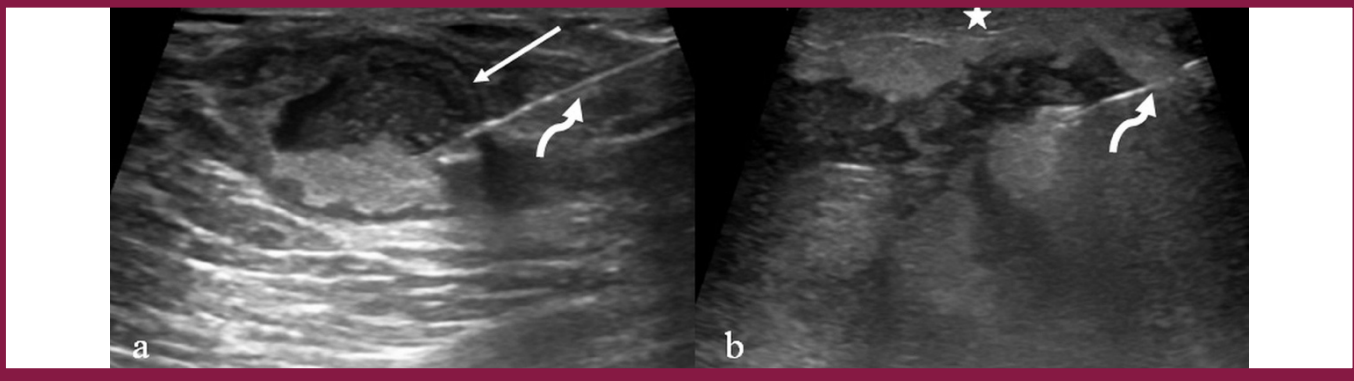

Figure 1. In a 28-year-old patient who was histopathologically diagnosed with idiopathic granulomatous mastitis, a complicated cyst (arrow) with dense floating debris and edema (star) on the skin are observed in the images obtained during US-guided biopsy (curved arrow)
US: Ultrasonography

was absent in the majority (78.6% and 66.7%, respectively) (Table 2).

DC-MRI findings (n=42) also showed left-sided (57.1%), non-mass (59.5%) lesions, often irregular in shape (66.7%). Diffusion restriction (100.0%), reactive lymph nodes (95.2%), and edema (90.5%) were frequently observed, with minimal edema in 61.9% of the cases (Figure 3). Notably, nipple retraction or fistula to the skin was absent in 57.1% and 69.0% of lesions, respectively (Table 3).

BPEs were minimal in 66.6% of cases. NME internal patterns were predominantly heterogeneous (48.3%) or clustered (44.8%) with regional (44.8%), multiple regional (20.7%), or segmental (20.7%) distributions (Figures 4, 5) (Table 3).

Median values for abscess size, lymph node short axis, and ADC were 25 mm, 10 mm, and ($1.064x10^{-3}$ mm^2/s), respectively, while the mean lymph node long axis was 18.0 mm (Table 3).

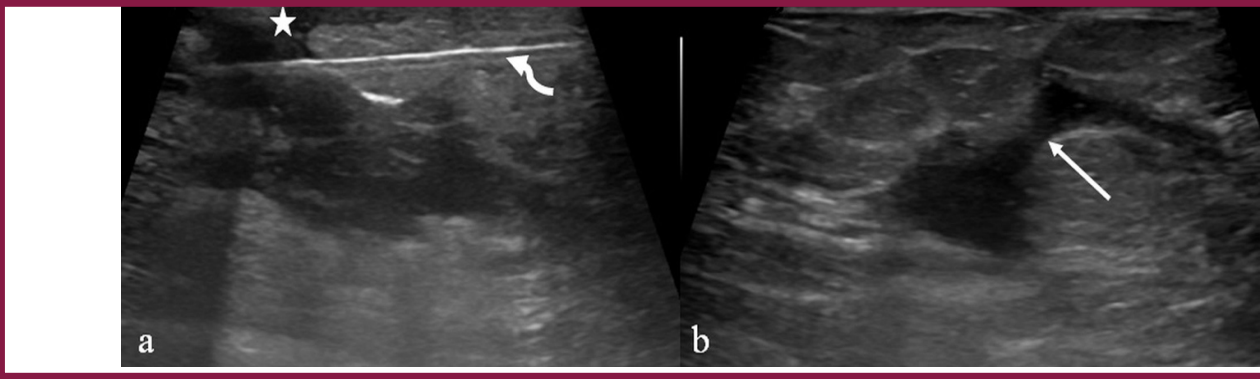

Figure 2. Images of a 25-year-old patient diagnosed with IGM obtained during the US-guided biopsy procedure (curved arrow) show a dense collection of skin fistulization (star), connecting tracts, and tubular extension (arrow)
IGM: Idiopathic granulomatous mastitis, US: Ultrasonography

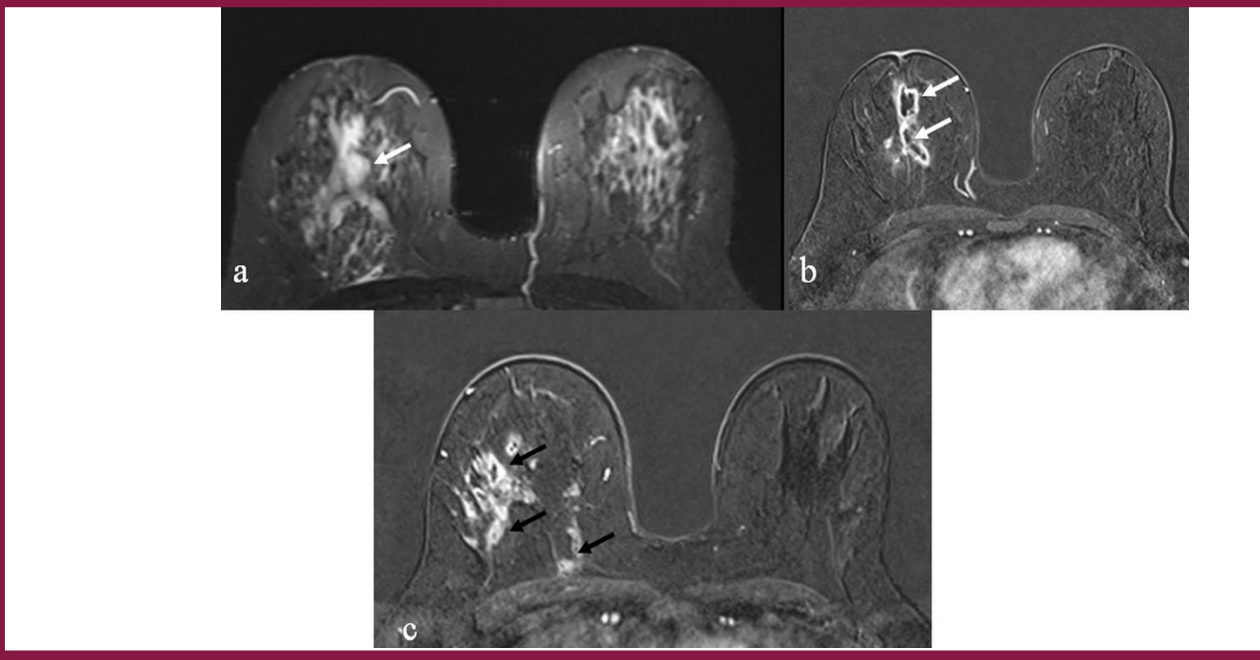

Figure 3. In the dynamic contrast-enhanced MRI examination of a 38-year-old female patient diagnosed with IGM, macro (white arrow) and microabscess foci (black arrow) are observed in the nonmassive enhancement area in the T2W fat-suppressed series (a) and postcontrast dynamic series (b, c)
MRI: Magnetic resonance imaging, IGM: Idiopathic granulomatous mastitis

Discussion

The results of our study indicate that the most commonly observed findings on US in patients diagnosed with IGM include indistinct margins characterized by a hypo-heterogeneous echo pattern, tubular extensions and connections, and the presence of cystic components containing floating debris. Furthermore, our analysis of MRI images in patients with IGM revealed a predominance of localized collections of abscesses or micro-abscesses, heterogeneous or clustered internal patterns, and NMEs exhibiting a regional distribution across most lesions. These findings underscore the diagnostic value of both US and MRI in the evaluation and characterization of IGM.

IGM generally affects young women of childbearing age (32-34 years) (2,6,13,14,15,16), while some reports indicate a wider age distribution ranging from late childhood to the late postmenopausal period (17,18). Likewise, the median age of our patients was 39 years, while 57.1% and 76.2% of patients were under 40 and 50 years of age, respectively. In addition, majority (95.2%) of our patients reported complaints such as breast pain, swelling, and rash, consistent with the most frequently reported manifestations of IGM (i.e., erythema, edema, sensitive-palpable unilateral breast mass, ulceration, discharge) (5,19). In addition, supporting the association between IGM and history of pregnancy and lactation (2), 40.5% of our patients reported a history of pregnancy and 23.8% had elevated serum levels of prolactin.

The majority of our patients had breast lesions considered to be probably benign (BI-RADS category 3, 38.1%) or with low suspicion of malignancy (BI-RADS category 4A, 40.5%). Likewise, IGM imaging studies have

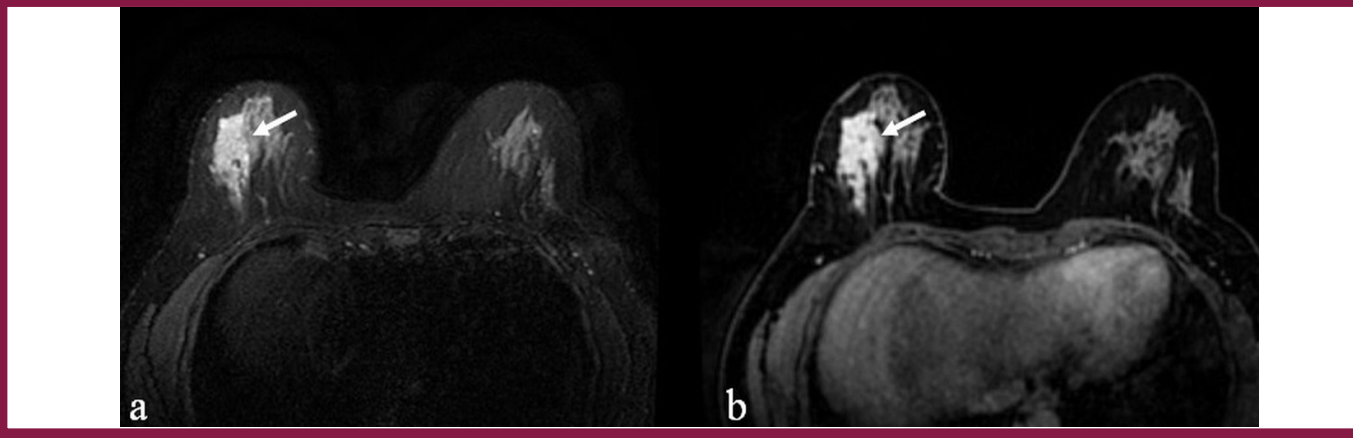

Figure 4. In the DC-MR images of a 40-year-old female patient diagnosed with IGM, a spicular contoured mass (arrow) is observed in the right breast, which is hyperintense in the T2W fat-suppressed series (a) and in postcontrast dynamic displays (b) with intense homogeneous contrast enhancement
IGM: Idiopathic granulomatous mastitis, DC-MR: Dynamic contrast-enhanced magnetic resonance

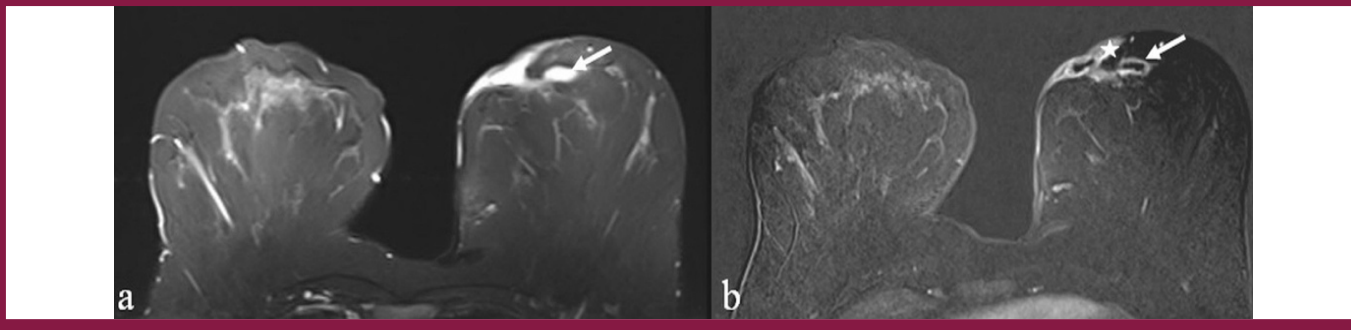

Figure 5. In the T2W fat-suppressed series (a) and postcontrast dynamic series (b) of a 42-year-old female patient diagnosed with IGM, mammary skin thickening (star) and abscess foci (arrow) with fistulization of the skin in the periareolar area are observed
IGM: Idiopathic granulomatous mastitis

indicated a higher prevalence of BI-RADS 3 (82.8% on MR, 55.2% on conventional methods) or BI-RADS 4 (3.4% on MRI and 37.9% on conventional methods) lesions (8).

Considering the imaging findings, representing the largest patient series for IGM in the literature, our findings revealed that breast US imaging and DC-MRI findings were consistent

Table 2. Breast US imaging findings (n=42)

US imaging findings, n (%)		
Lesion side	Right	18 (42.9)
	Left	22 (52.4)
	Bilateral	2 (4.8)
Localization	Retrosternal	2 (4.8)
	1-3 quadrant	28 (66.7)
	Diffuse	12 (28.6)
Lesion type	Mass	13 (31.0)
	Non-mass	29 (69.0)
Lesion shape	Oval-round	4 (9.5)
	Irregular	38 (90.5)
Lesion echo pattern	Hypo-heterogenic	39 (92.9)
	Echogenic-heterogenic	3 (7.1)
Lesion margin	Well-circumscribed lesion	3 (7.1)
	Indeterminate lesion	37 (88.1)
	Spiculated lesion	2 (4.8)
Fistula to the skin	Absent	28 (66.7)
	Present	14 (33.3)
Cystic component	Absent	13 (31.0)
	Present	29 (69.0)
Floating debris	Absent	15 (35.7)
	Present	27 (64.3)
Ductal ectasia	Absent	20 (47.6)
	Ipsilateral	11 (26.2)
	Contralateral	8 (19.0)
	Bilateral	3 (7.1)
Skin thickening	Absent	4 (9.5)
	Present	38 (90.5)
Edema	Absent	2 (4.8)
	Present	40 (95.2)
Reactive lymph nodes	Absent	2 (3.8)
	Present	40 (95.2)
Nipple retraction	Absent	33 (78.6)
	Present	9 (21.4)
Tubular extension and connecting tracts	Absent	5 (11.9)
	Present	37 (88.1)

US: Ultrasonography

Table 3. Breast DC-MRI findings (n=42)

Breast DC-MRI findings, n (%)		
Lesion side	Right	16 (38.1)
	Left	24 (57.1)
	Bilateral	2 (4.8)
Localization	Retrosternal	11 (26.2)
	1-3 quadrant	19 (45.2)
	Diffuse	12 (28.6)
Lesion type	Mass	17 (40.5)
	Non-mass	25 (59.5)
Lesion shape	Oval-round	14 (33.3)
	Irregular	28 (66.7)
Fistula to the skin	Absent	29 (69.0)
	Present	13 (31.0)
Microabscess	Absent	19 (46.3)
	Present	22 (53.7)
Localized collective abscess	Absent	17 (42.5)
	Present	23 (57.5)
Abscess size (mm), median (min.-max.)		25 (0-62)
Skin thickening	Absent	20 (47.6)
	Present	22 (52.4)
Edema	Absent	4 (9.5)
	Minimal	26 (61.9)
	Moderate	11 (26.2)
	Massive	1 (2.4)
Lymph node long axis (n=33, cm), mean (SD)		18.0 (6.8)
Lymph node short axis (n=31, cm), median (min.-max.)		10 (6-21)
Reactive lymph nodes	Absent	2 (3.8)
	Present	40 (95.2)
Nipple retraction	Absent	24 (57.1)
	Present	18 (42.9)
BPEs (n=33)	Minimal	22 (66.6)
	Moderate	6 (18.2)
	Intense	5 (15.2)
NME internal pattern (n=29)	Heterogenic	14 (48.3)
	Homogeny	2 (6.9)
	Cluster	13 (44.8)
NME distribution type (n=29)	Regional	13 (44.8)
	Diffuse	3 (10.3)
	Focal	1 (3.4)
	Multiple regional	6 (20.7)
	Segmental	6 (20.7)
Diffusion restriction	Absent	0 (0.0)
	Present	42 (100.0)
ADC value (x10^{-3} mm^2/s), median (min.-max.)		1.064 (650-1.580)

ADC: Apparent diffusion coefficient, BPE: Background parenchymal enhancements, DC-MRI: Dynamic contrast-enhanced magnetic resonance imaging, NME: Non-mass enhancement, SD: Standard deviation, min.: Minimum, max.: Maximum

in terms of identifying the left-sided (52.4% and 57.1%, respectively), non-mass (69.0% and 59.5%), and irregularly shaped (90.5% and 66.7%) lesions located in the 1-3 quadrant (66.7% and 45.2%) in most patients. The most prevalent associated findings on both US and DC-MRI were the presence of edema (95.2% and 90.5%), reactive lymph nodes (95.2% for each), and skin thickening (90.5% and 52.4%) along with the presence of nipple retraction (42.9% and 21.4%) or fistula to skin (66.7% and 69.0%) in most patients.

US-specific findings in our series indicated lesions with indeterminate margins (88.1%) and hypo-heterogeneous echo pattern (92.9%) in addition to the presence of tubular extension and connecting tracts (88.1%), cystic component (69.0%), floating debris (64.3%), and ductal ectasia (52.4%) in most patients. DC-MRI-specific findings indicated localized collective abscess (57.5%) and micro-abscess (53.7%), as well as minimal BPEs (66.6%) and NMEs with heterogeneous (48.3%) or cluster (44.8%) internal pattern and a regional distribution (44.8%) in most lesions.

Similarly, in a radiological investigation involving 36 patients diagnosed with IGM, the predominant observations on breast US imaging included a heterogeneously hypoechoic mass displaying an irregular shape and indistinct margin (72.2%), tubular extension with connecting tracts, and tunneling around the lesions (50.0%). In addition, fluid collection with floating debris accounted for 27.8% of cases, and anechoic cystic components were observed in 13.9% of cases. The authors also highlighted two novel imaging indicators of IGM, namely duct ectasia containing secretion and a high-flow pseudocyst appearance (6).

In line with our US-based findings in IGM lesions, irregular hypoechoic lesions with tubular extensions (indicating the insinuating rather than destroying effect of IGM on breast lobules) are considered the most frequently reported US imaging findings in patients with IGM, whereas isolated ill-defined hypoechoic or heterogeneous lesions are the second most common finding (3,8,20,21,22,23,24). The ancillary US imaging findings reported in studies among patients with IGM are variable, including parenchymal edema, skin thickening, fluid collection, and axillary lymphadenopathy (2,4,8,13,20,22,24,25,26,27).

While studies investigating the MRI features of IGM also indicate a variable set of findings depending upon the severity of inflammation, heterogeneous ill-defined masses and segmental-regional NMEs are identified in most cases, and NME lesions are more frequent than mass-like lesions, in line with our findings (4,5,8,12,13,20,24,26,28,29).

Prediagnosis imaging observations in 29 patients with IGM revealed heterogeneous hypoechoic lesions with tubular extensions in 55.2% of cases, mild to moderately enlarged axillary lymph nodes in 41.4%, and fistula tracts in 10.3% of cases on US. MRI findings indicated the involvement of multiple quadrants (52.2%), heterogeneous segmental and regional NME, enlarged axillary lymph nodes (52.2%), and abscesses with marked peripheral ring enhancement (86.2%), suggesting edematous inflammation in the peripheral parenchyma (8). In a retrospective study of 20 patients with IGM, MRI identified a total of 29 lesions, with 14 appearing as mass enhancements and the remaining 15 characterized as NMEs with segmental distribution (40%) and diverse enhancement patterns (53%) (13). Analyzing DC-MRI results in 39 patients with IGM, the authors reported significantly lower ADC values for the lesion compared with the contralateral normal parenchyma, with NME and abscess noted in 92.3% and 33.3% of patients, respectively (12).

Similarly, our study predominantly observed regional distribution (44.8%) and heterogeneous enhancement patterns (48.3%) in the NME lesions, coupled with localized collective abscess (57.5%) and micro-abscess (53.7%). Furthermore, the presence of diffusion restriction in all lesions and the median ADC values ($1.064x10^3$ mm^2/s) in our analysis align with data from IGM imaging studies indicating restricted diffusion in the affected parenchyma, consistently yielding lower mean ADC values ($1.0x10^3$ mm^2/s) than those observed in normal breast parenchyma ($2.3x10^3$ mm^2/s) (4,30). However, despite the likely impact of the chronic inflammatory response in IGM on reducing water diffusion capacity and relative ADC values (4), the diminished ADC sequence signal in diffusion-weighted imaging in IGM is considered to play a minimal role in distinguishing it from inflammatory breast cancer (14,31).

In our study, BPEs were minimal in most patients, and segmental enhancements were noted in only 20.7% of patients. In contrast, some studies reported segmental heterogeneous enhancements and rim enhancement features rather than regional distribution as the most commonly encountered MRI findings of IGM lesions (8,9,13,26,32,33,34). Notably, segmental enhancements are considered to be features of ductal carcinoma *in situ* on MRI (35). In addition, although IGM is a benign pathology showing non-mass-like lesions with restricted diffusion, it may also show clustered ring-like enhancement similar to malignant lesions (9,12,13,32).

In our study, the most prevalent associated findings on both US and DC-MRI were the presence of edema (95.2% and 90.5%), reactive lymph nodes (95.2% for each), and skin thickening (90.5% and 52.4%). Along with the findings of floating debris (64.3%) on US and localized collective abscess (57.5%) and micro-abscess (53.7%) on DC-MRI, the imaging findings of IGM in the current study support the consideration of parenchymal heterogeneity with abscess formation and axillary lymphadenopathy as well as focal mastitis with interstitial edema to favor an inflammatory

granulomatous process (3,16,31). Indeed, associated diffuse parenchymal edema, which is a well-known feature of IGM (33), as well as associated lesions such as microabscesses or larger fluid collections in advanced cases (4,20,24) are considered likely to play a role in volume enlargement of the affected breast related to IGM (10).

Our results corroborate the established notion that skin thickening is a frequently observed imaging characteristic in IGM, evident in more than 90% of cases (27,34). Conversely, the involvement of the nipple and nipple-areolar complex is infrequent (4,10), and sinus tracts extending to the skin surface may become apparent in cases of delayed diagnosis or a history of prior intervention (4,20,22,32).

A collection of imaging features plays a role in the differential diagnosis of IGM, such as an indistinct mass with the long axis of the lesion parallel to the chest wall and multifocal abscess cavities on US. Infective mastitis, on the other hand, exhibits characteristics like diffuse or focal skin thickening, inhomogeneous breast tissue with or without an irregular hypoechoic mass, and fluid collection on US. Malignancy is distinguished by skin thickening and breast edema with dilated lymphatics on US, along with extensive NME featuring areas of a clustered ring-like pattern or contiguous irregular breast masses with rapid enhancement on MRI (2,11,35). Our imaging findings underscore the capability of US to propose an IGM diagnosis in a suitable clinical context (6), while MRI can aid in the differential diagnosis and evaluation of disease extent in patients with inconclusive conventional findings (4,8). Nevertheless, a definitive histopathological diagnosis is deemed indispensable for IGM before any surgical procedures are considered (3,5).

Indeed, MRI or DC-MRI was also considered not discriminatory in differentiating IGM from inflammatory carcinoma because of overlapping signs of inflammation and intense early enhancement (3). However, MRI-enhanced imaging has higher accuracy in assessing the extent of lesions compared with US imaging alone or combined with mammography (31).

Hence, MRI is a supplementary instrument that enhances the visibility of lesions not adequately visualized by conventional imaging modalities because of parenchymal edema. It aids in ruling out a diagnosis of inflammatory breast cancer (3,5,24) and functions as a subsequent imaging tool for diseases that are diffuse, aggressive, and non-responsive (4,5,8,20,31).

Study Limitations

The comprehensive presentation of breast US imaging and DC-MRI findings in the largest patient series for IGM in the literature seems to be the major study strength. However, our study has certain limitations. First, the potential lack of generalizability is an important limitation due to the relatively small sample size. Second, lack of data on other inflammatory breast pathologies considered in the differential diagnosis of IGM as well as more comprehensive data on socioeconomic characteristics and breastfeeding history and their relation to US-MRI findings seem to be another limitation that would otherwise extend the knowledge achieved in the current study.

Conclusion

In our series of IGM, both breast US imaging and DC-MRI commonly revealed non-mass lesions with irregular shapes, accompanied by edema, reactive lymph nodes, and skin thickening in the majority of patients. Noteworthy US-specific findings included a hypoheterogeneous echo pattern, tubular extension and connecting tracts, cystic components, floating debris, and ductal ectasia. On the other hand, DC-MRI-specific findings predominantly featured localized collective abscesses or microabscesses, minimal BPEs, and NMEs with heterogeneous or clustered internal patterns and a regional distribution in most lesions. Our findings underscore the diagnostic significance of US in an appropriate clinical context, particularly when complemented by MRI for aiding differential diagnosis. However, it is essential to emphasize that histopathology remains the cornerstone for the definitive diagnosis and appropriate management of IGM.

Ethics

Ethics Committee Approval: This study was conducted in accordance with the ethical principles stated in the "Declaration of Helsinki" and approved by Recep Tayyip Erdoğan University Hospital Non-interventional Clinical Research Ethics Committee (date: 21/01/2021; protocol number: 2021/18).

Informed Consent: Written informed consent was obtained from all patients.

Authorship Contributions

Surgical and Medical Practices: F.T., N.O.M., E.T., Concept: F.T., Y.M., M.G.G., Design: Y.M., N.O.M., M.G.G., E.T., Data Collection or Processing: F.T., N.O.M., E.T., Analysis or Interpretation: Y.M., M.G.G., E.T., Literature Search: Y.M., N.O.M., M.G.G., Writing: F.T.

Conflict of Interest: xxxxxx

Financial Disclosure: xxxxxx

References

1. Kessler E, Wolloch Y. Granulomatous mastitis: a lesion clinically simulating carcinoma. Am J Clin Pathol. 1972;58:642-646. [Crossref]
2. Pluguez-Turull CW, Nanyes JE, Quintero CJ, Alizai H, Mais DD, Kist KA, et al. Idiopathic granulomatous mastitis: manifestations at multimodality imaging and pitfalls. Radiographics. 2018;38:330-356. [Crossref]
3. Sripathi S, Ayachit A, Bala A, Kadavigere R, Kumar S. Idiopathic granulomatous mastitis: a diagnostic dilemma for the breast radiologist. Insights Imaging. 2016;7:523-529. [Crossref]
4. Fazzio RT, Shah SS, Sandhu NP, Glazebrook KN. Idiopathic granulomatous mastitis: imaging update and review. Insights Imaging. 2016;7:531-539. [Crossref]
5. Durur-Subasi I. Diagnostic and interventional radiology in idiopathic granulomatous mastitis. Eurasian J Med. 2019;51:293-297. [Crossref]
6. Alikhassi A, Azizi F, Ensani F. Imaging features of granulomatous mastitis in 36 patients with new sonographic signs. J Ultrasound. 2020;23:61-68. [Crossref]
7. Bashir MU, Ramcharan A, Alothman S, Beaugris S, Khan SA, Sbeih MA, et al. The enigma of granulomatous mastitis: A series. Breast Dis. 2017;37:17-20. [Crossref]
8. Oztekin PS, Durhan G, Nercis Kosar P, Erel S, Hucumenoglu S. Imaging Findings in patients with granulomatous mastitis. Iran J Radiol. 2016;13:e33900. [Crossref]
9. Dursun M, Yilmaz S, Yahyayev A, Salmaslioglu A, Yavuz E, Igci A, et al. Multimodality imaging features of idiopathic granulomatous mastitis: Outcome of 12 years of experience. Radiol Med. 2012;117:529-538. [Crossref]
10. Soylu Boy FN. MR Imaging evaluation of the volume changes and the signs of deformation in the breasts with granulomatous mastitis. Bosphorus Med J. 2022;9:127-131. [Crossref]
11. Matich A, Sud S, Buxi TBS, Dogra V. Idiopathic granulomatous mastitis and its mimics on magnetic resonance imaging: a pictorial review of cases from India. J Clin Imaging Sci. 2020;10:53. [Crossref]
12. Aslan H, Pourbagher A, Colakoglu T. Idiopathic granulomatous mastitis: magnetic resonance imaging findings with diffusion MRI. Acta Radiol. 2016;57:796-801. [Crossref]
13. Poyraz N, Emlik GD, Batur A, Gundes E, Keskin S. Magnetic resonance imaging features of idiopathic granulomatous mastitis: a retrospective analysis. Iran J Radiol. 2016;13:e20873. [Crossref]
14. Yilmaz R, Demir AA, Kaplan A, Sahin D, Ozkurt E, Dursun M, et al. Magnetic resonance imaging features of idiopathic granulomatous mastitis: is there any contribution of diffusion-weighted imaging in the differential diagnosis? Radiol Med. 2016;121:857-866. [Crossref]
15. Al-Khaffaf B, Knox F, Bundred NJ. Idiopathic granulomatous mastitis: a 25-year experience. J Am Coll Surg. 2008;206:269-273. [Crossref]
16. Kok KY, Telisinghe PU. Granulomatous mastitis: presentation, treatment and outcome in 43 patients. Surgeon. 2010;8:197-201. [Crossref]
17. Lai EC, Chan WC, Ma TK, Tang AP, Poon CS, Leong HT. The role of conservative treatment in idiopathic granulomatous mastitis. Breast J. 2005;11:454-456. [Crossref]
18. Bani-Hani KE, Yaghan RJ, Matalka II, Shatnawi NJ. Idiopathic granulomatous mastitis: time to avoid unnecessary mastectomies. Breast J. 2004;10:318-322. [Crossref]
19. Ocal K, Dag A, Turkmenoglu O, Kara T, Seyit H, Konca K. Granulomatous mastitis: clinical, pathological features, and management. Breast J. 2010;16:176-182. [Crossref]
20. Gautier N, Lalonde L, Tran-Thanh D, El Khoury M, David J, Labelle M, et al. Chronic granulomatous mastitis: Imaging, pathology and management. Eur J Radiol. 2013;82:165-175. [Crossref]
21. Memis A, Bilgen I, Ustun EE, Ozdemir N, Erhan Y, Kapkac M. Granulomatous mastitis: imaging findings with histopathologic correlation. Clin Radiol. 2002;57:1001-1006. [Crossref]
22. Hovanessian Larsen LJ, Peyvandi B, Klipfel N, Grant E, Iyengar G. Granulomatous lobular mastitis: imaging, diagnosis, and treatment. AJR Am J Roentgenol. 2009;193:574-581. [Crossref]
23. Sabaté JM, Clotet M, Gómez A, De Las Heras P, Torrubia S, Salinas T. Radiologic evaluation of uncommon inflammatory and reactive breast disorders. Radiographics. 2005;25:411-424. [Crossref]
24. Alsaleh N. Assertive clinical practice in managing patients with idiopathic granulomatous mastitis: Review of literature. Ann Med Surg (Lond). 2021;70:102792. [Crossref]
25. Aghajanzadeh M, Hassanzadeh R, Alizadeh Sefat S, Alavi A, Hemmati H, Esmaeili Delshad MS, et al. Granulomatous mastitis: presentations, diagnosis, treatment and outcome in 206 patients from the north of Iran. Breast. 2015;24:456-460. [Crossref]
26. Al-Khawari HA, Al-Manfouhi HA, Madda JP, Kovacs A, Sheikh M, Roberts O. Radiologic features of granulomatous mastitis. Breast J. 2011;17:645-650. [Crossref]
27. Lee JH, Oh KK, Kim EK, Kwack KS, Jung WH, Lee HK. Radiologic and clinical features of idiopathic granulomatous lobular mastitis mimicking advanced breast cancer. Yonsei Med J. 2006;47:78-84. [Crossref]
28. Ozturk M, Mavili E, Kahriman G, Akcan AC, Ozturk F. Granulomatous mastitis: radiological findings. Acta Radiol. 2007;48:150-155. [Crossref]
29. Zhao Q, Xie T, Fu C, Chen L, Bai Q, Grimm R, et al. Differentiation between idiopathic granulomatous mastitis and invasive breast carcinoma, both presenting with non-mass enhancement without rim-enhanced masses: The value of whole-lesion histogram and texture analysis using apparent diffusion coefficient. Eur J Radiol. 2020;123:108782. [Crossref]
30. Abowarda MH, Hasan DI, Elteeh OA. Prepredictive value of ADC mapping in discriminating probably benign and suspicious breast lesions. Egypt J Radiol Nucl Med. 2015;46:545-551. [Crossref]
31. Yuan QQ, Xiao SY, Farouk O, Du YT, Sheybani F, Tan QT, et al. Management of granulomatous lobular mastitis: an international multidisciplinary consensus (2021 edition). Mil Med Res. 2022;9:20. [Crossref]
32. Kocaoglu M, Somuncu I, Ors F, Bulakbasi N, Tayfun C, Ilkbahar S. Imaging findings in idiopathic granulomatous mastitis. A review with emphasis on magnetic resonance imaging. J Comput Assist Tomogr. 2004;28:635-641. [Crossref]
33. Yildiz S, Aralasmak A, Kadioglu H, Toprak H, Yetis H, Gucin Z, et al. Radiologic findings of idiopathic granulomatous mastitis. Med Ultrason. 2015;17:39-44. [Crossref]
34. Mossa-Basha M, Fundaro GM, Shah BA, Ali S, Pantelic MV. Ductal carcinoma in situ of the breast: MR imaging findings with histopathologic correlation. Radiographics. 2010;30:1673-1687. [Crossref]
35. Wang L, Wang D, Fei X, Ruan M, Chai W, Xu L, et al. A rim-enhanced mass with central cystic changes on MR imaging: how to distinguish breast cancer from inflammatory breast diseases? PLoS One. 2014;9:e90355. [Crossref]